

MIT Open Access Articles

The Nature of Heat Release in Gasoline PPCI Engines

The MIT Faculty has made this article openly available. **Please share** how this access benefits you. Your story matters.

Citation: Sang, Wenwen, Wai K. Cheng, and Amir Maria. "The Nature of Heat Release in Gasoline PPCI Engines." SAE Technical Paper Series (April 1, 2014).

As Published: <http://dx.doi.org/10.4271/2014-01-1295>

Publisher: SAE International

Persistent URL: <http://hdl.handle.net/1721.1/98045>

Version: Author's final manuscript: final author's manuscript post peer review, without publisher's formatting or copy editing

Terms of use: Creative Commons Attribution-Noncommercial-Share Alike



The Nature of Heat Release in Gasoline PPCI Engines

Author, co-author (**Do NOT enter this information. It will be pulled from participant tab in MyTechZone**)

Affiliation (**Do NOT enter this information. It will be pulled from participant tab in MyTechZone**)

Copyright © 2014 SAE International

Abstract

The heat release characteristics in terms of the maximum pressure rise rate (MPRR) and combustion phasing in a partially premixed compression ignition (PPCI) engine are studied using a calibration gasoline. Early port fuel injection provides a nearly homogeneous charge, into which a secondary fuel pulse is added via direct injection (DI) to provide stratification which is affected by the timing of the start of injection (SOI). As the SOI the DI fuel is retarded from early compression, MPRR first decreases, then increases substantially, and decreases again. The MPRR correlates mostly with the combustion phasing. The SOI timing plays an indirect role. The observation is explained by a bulk heat release process of which the rate increases with temperature rather than by a sequential ignition process. Observations from compression ignition of representative homogeneous charges in a Rapid Compression Machine support this explanation.

Introduction

Gasoline engines running in the partially premixed compression ignition mode have the potential of high efficient and low emissions at high load [1-4]. Fuel is injected into the cylinder during the compression process and combustion behavior is affected by the injection timing [1, 2]. The incomplete mixing of the injected fuel provides a stratification which could relax the maximum pressure rise rate (MPRR) encountered in homogeneous charge compression ignition (HCCI) engines under high load [3, 4]. The nature of heat release in these PPCI engine, however, has not been well defined. The conventional wisdom is that combustion takes place in a progressive manner through the sequential ignition of the mixture along the concentration and/or temperature gradients. The purpose of this paper is to examine, through the response of a PPCI engine to the sweep of direct injection timing, the validity of this description.

It should be noted that the PPCI combustion discussed in this paper is specifically for partially premixed charge from a single fuel – gasoline, and with split injection to control stratification. The premise is that the long ignition delay and ease of vaporization of the early port-fuel-injected gasoline would provide a background charge which is nearly homogeneous. Then a second late injection close to TDC would provide the charge stratification to control the heat release rate [1]. As

such, the combustion phenomena studied here are different from the PPCI work using diesel fuel [5, 6], for which the vaporization and ignition delays are very different; from using single injection [7], for which the emphasis is not on putting a pilot fuel over a background nearly homogeneous charge; and from using dual fuels such as the reactivity controlled compression ignition (RCCI) concept [8-10], for which the reactivity of the local charge is controlled by using two fuels of different reactivity.

Experimental

Engine

A production Renault/ Mitsubishi F9Q B800 common rail diesel engine that has been modified is used in this study. The set up details have been described previously [11]. The compression ratio is lowered to 15 by putting in a spacer between the head and the block. Engine specifications are given in Table 1.

Table 1. Engine Specification

Description	Specification
Arrangement	In-line 4 modified for single cylinder operation
Displacement per cylinder	467.5 cc
Bore x stroke	80mm x 93 mm
Compression ratio	15
Intake valve opening	3° BTDC
Intake valve closing	21° ABDC
Exhaust valve opening	46° BBDC
Exhaust valve closing	6° BTDC
Fuel injection	DI + PFI

The engine is converted to run under single cylinder operation to eliminate issues with cylinder variations. Separate intake and exhaust runners are created for the firing cylinder, while the original manifolds are modified to connect to only the non-firing cylinders.

The original turbocharger connected to the engine is removed. In its place, a separate intake air system employing a screw type supercharger with bypass to control the airflow is connected to the intake of the firing cylinder. The system is designed to operate from 1 to 2 bar absolute pressure. The intake air temperature is controlled by a heater to a range of 40° to 140° C independent of engine operation.

A certification gasoline (Halterman 437) with RON of 97 is used for all experiments. To study charge stratification effects, the engine employs two fuel injection systems that could be used separately or simultaneously. For the common rail direct injection that comes with the engine, injection pressure is at 490 bar. A port fuel injector, with a separate fuel tank, is added at the intake runner targeting the back of the intake valve. The port fuel injection (PFI) pressure is set to 2.7 bar gauge. To prevent formation of bubbles, all fuel returns are cooled through a heat exchanger (with ice water) before going back to the fuel tank. The fuel temperatures, however, are not regulated.

Rapid Compression Machine

A Rapid Compression Machine (RCM) is used to characterize the compression ignited combustion behavior of a homogeneous mixture [12]. A schematic of the machine is shown in Figure 1. Table provides the key specifications and dimensions of the RCM. The compression ratio could be changed easily by changing the head piece, thereby changing the clearance volume. In this manner, the compression temperature could be changed quickly without changing the machine wall temperature which takes a long time to equilibrate.

Table 2. RCM Specification

Combustion Piston Diameter [m]	0.0508
Stroke [m]	0.2032
Compression Ratio	8-20
Maximum Initial RCM Pressure [bar absolute]	2.6
Maximum Initial RCM Temperature [°C]	100

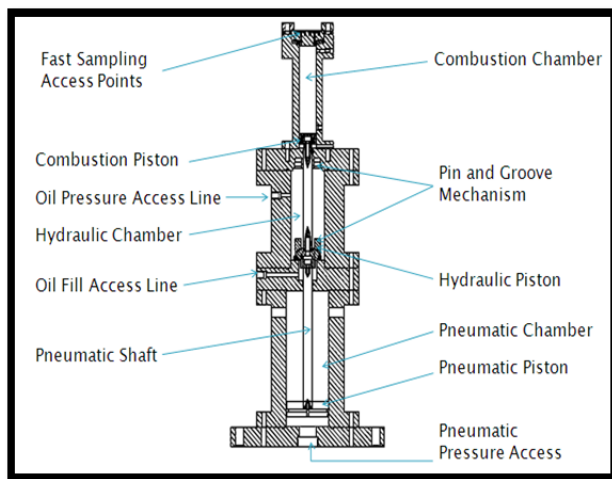


Figure 1. Schematic of RCM.

To ensure a uniform mixture with a definite composition, the fuel-air mixture is prepared in a separate chamber, referred to as the Mixture Preparation Unit (MPU) before being admitted into the RCM. Gas species are metered via the partial pressures. Liquid fuel is metered using a calibrated syringe. There is a mixing fan in the MPU to obtain a homogeneous mixture. The shaft of the fan is coupled to a motor outside the MPU via a vacuum feed through.

The volume of the MPU is approximately 10 times larger than the combustion chamber. The maximum pressure is approximately 3 bars, which is limited by the maximum

absolute pressure reading achievable and the leak rate of the vacuum feed-through. Depending on the amount of mixture admitted into the RCM, one batch can typically last for approximately 10 runs. All of the surfaces of the MPU are heated to ensure that the liquid fuel fully vaporizes. The required temperature is determined based on the amount of fuel that is being admitted and its dew point.

Results

The results reported here are for the engine of 15:1 compression ratio operating with Halterman 437 fuel (RON=97/MON=89) at 1200 rpm. The intake pressure is at 1.8 bar; the exhaust pressure is at 1.9 bar. The intake temperature is regulated at 80° C. EGR varies from 0 to 20%. The total fuel per cycle is fixed at 23 mg. The nominal Φ based on fuel and intake air ranges from 0.4 to 0.5 as the EGR changes, with the fuel amount kept constant. The nominal GIMEP is 10 bar; see Figure 2. The nominal gross indicated efficiency is 47%. The experimental conditions are summarized in Table 2.

Table 3. Experimental conditions

Engine speed (rpm)	1200
Intake/exhaust pressure (bar)	1.8/1.9
Intake/engine coolant temperature (° C)	80/80
Total (port + direct injection) fuel amount (mg)	23
EGR (%)	0,10,15,20
Nominal GIMEP (bar)	10

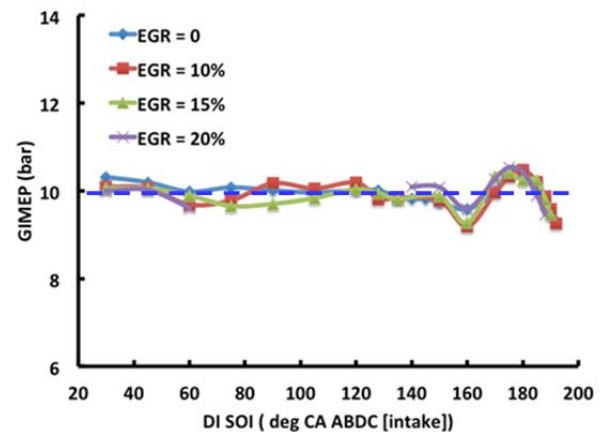


Figure 2 GIMEP versus direct injection timing; PFI/DI split of 60/40.

Split injection: PFI/DI 60/40 split

The first results shown are for the split injection case. The injection is divided between PFI and DI in a 60/40 split by fuel volume. (The same fuel is used for both PFI and DI.) The PFI injector provides an essentially homogeneous background charge. The DI injection, at pressure of 490 bar, has a duration of 390 μ s, which corresponds to 2.8 crank angle degrees. Thus the injection event is short compared to the compression and expansion processes. Each injection sweep has been done at a fixed level of EGR. As such, the combustion phasing and MPRR changes in the sweep.

The MPRR as a function of SOI of the direct injection pulse is shown in Figure 3. To simplify the discussion, the behavior at

EGR = 15% is discussed first. The corresponding cumulative mass fraction burn curves at selected points are also shown. As illustrated in Figure 3, there are three regimes (marked as A, B and C) for the MPRR behavior.

two-part release is quite evident in the mass fraction burned curve at point T; see Figure 3.

The pressure curves for the 3 regimes are shown in Figure 4. As injection is retarded, combustion retards correspondingly in regime A. Then the trend reverses as combustion advances with injection retard in regime B. Finally, the trend reverses again in regime C with further retard of injection, as the heat release progresses towards a two-part process.

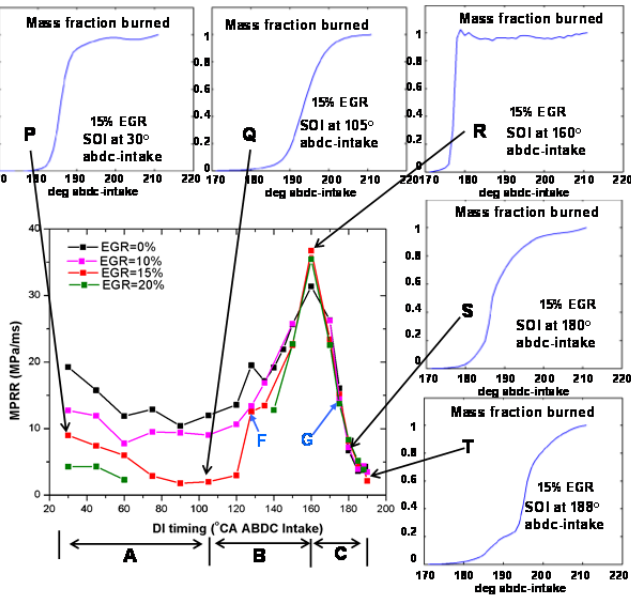


Figure 3 MPRR versus SOI of DI fuel. Fuel split is 60/40 by fuel volume. Engine operates at 1200 rpm, 10 bar nominal GIMEP. The associated mass fraction burned curves are for EGR=15%.

In regime A, as injection is retarded from P (at 30° ABDC-intake) to Q (at 105° ABDC-intake), the MPRR drops significantly (from 9 MPa/ms to 1.8 MPa/ms). The relaxing of the heat release rate can be seen by comparing the mass fraction burn curves at points P and Q. Note that heat release is significantly later in Q.

The behaviors for EGR = 0 and 10% are similar to those of EGR = 15%. At EGR = 20%, the decrease of MPRR is observed as SOI is retarded from 30° to 60° ABDC-intake; however, the combustion becomes erratic and ignition fails with further injection retard. When SOI is retarded beyond 140° ABDC-intake, the combustion stabilizes again. This point will be taken up in the discussion later.

In regime B, when injection is further retarded from Q, MPRR increases. The very high peak MPRR of 37 MPa/ms is achieved at point R. Comparing the mass burn curves of Q and R, combustion occurs progressively earlier in regime B with injection retard.

The MPRR behavior in regime B is similar for EGR = 0 to 15%. At EGR = 20%, however, combustion becomes unstable until SOI is at 140° ABDC-intake or beyond, at which combustion becomes stable again. This point will be taken up in the discussion section later.

In regime C, MPRR decreases with further retard of injection. When the direct injection is late, the heat release becomes more a two-part process. There is some evidence of the two-part heat release at point S, at which the mass fraction burned curve shows a slower burn first followed by a faster burn. The

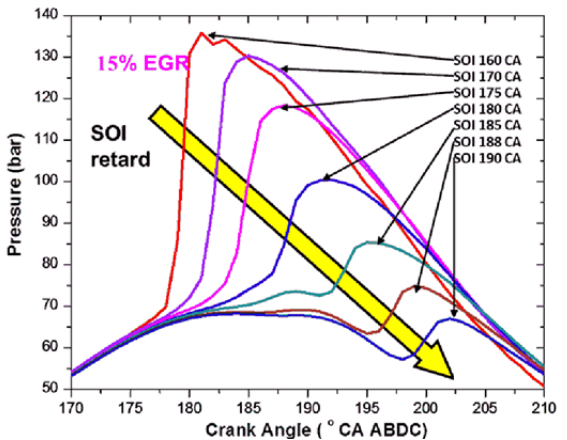
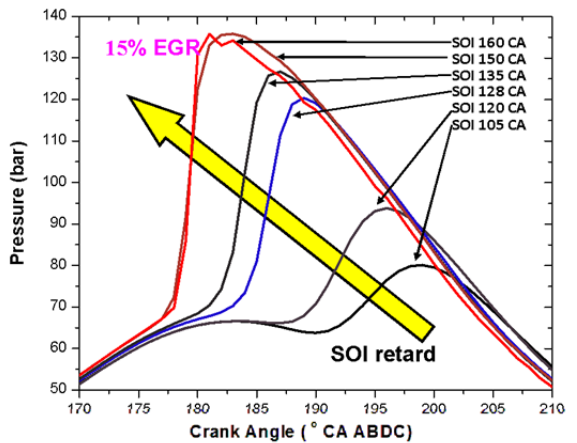
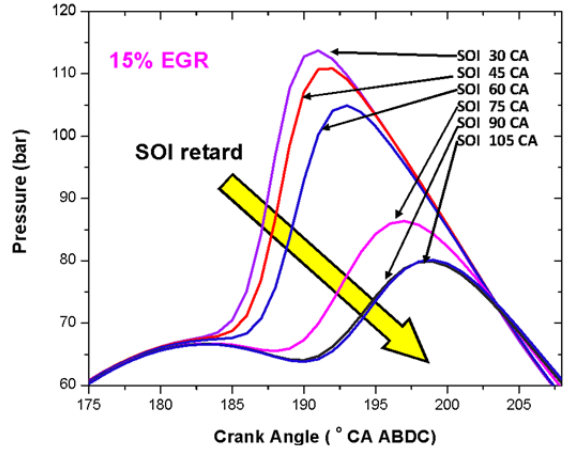


Figure 4 Pressure curves at different SOI of the DI fuel for the 3 regimes in Figure 3. The curves have been low-pass filtered at 4 KHz and averaged over 100 cycles. These filtered pressure traces are the ones used in the heat release analysis.

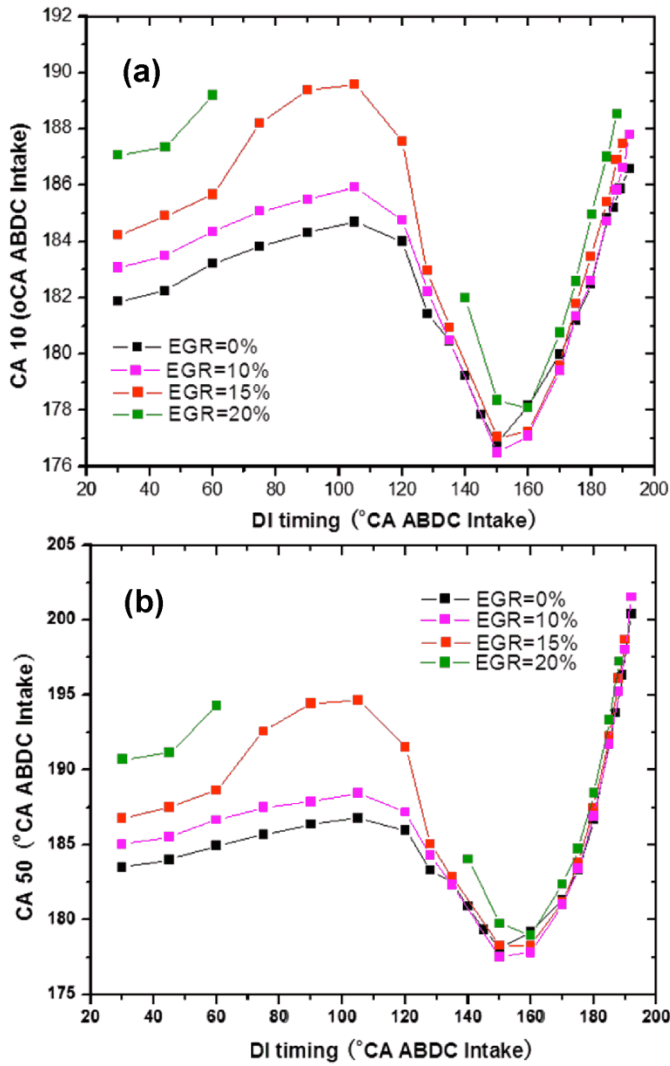


Figure 5 Combustion phasing as a function of SOI of direct injection; (a) CA10; (b) CA50.

The corresponding CA10 and CA50 values for the pressure traces in Figure 4 are shown in Figure 5.

That the heat release in regime C progresses towards a two part heat release process is demonstrated in the plot of CA50 versus CA10; see Figure 6. In regimes A and B (points P to Q to R), the CA50 values correlates with CA10. In regime C (points R to S to T), the curve begins to diverge from that of regimes A and B. This divergence is due to the fact that the second heat release occurs much later, especially for the late injection cases. For the SOI from point S to point T, the heat release actually starts before the fuel is injected; i.e. the PFI fuel is ignited first, followed by the later combustion of the DI fuel.

Similar divergence is observed for the other EGR cases; see Figure 7.

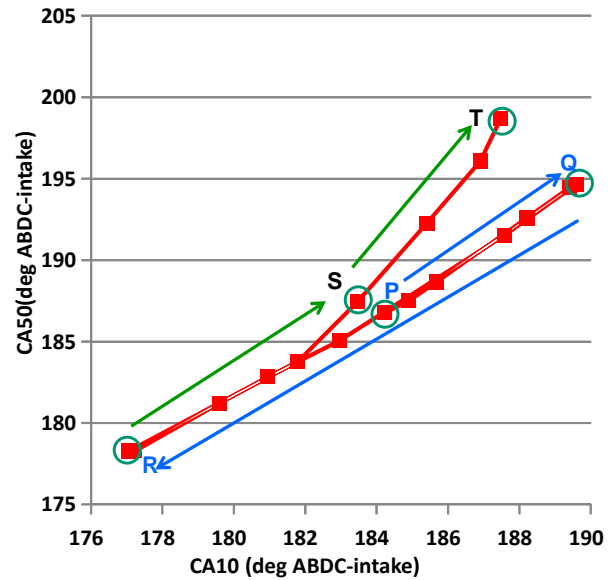


Figure 6 CA50 versus CA10 for the EGR=15% case of the data in Figure 3.

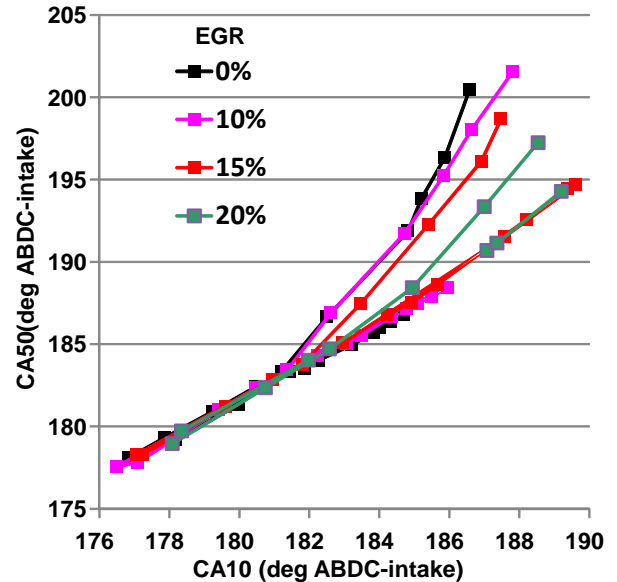


Figure 7 CA50 versus CA10 for all data in Figure 3.

The NO emissions are shown in Figure 8. The emission is negligible in regime A. High emission levels up to over 2000 ppm are observed in the high MPRR regions in regimes B and C. The high MPRR values suggest that combustion at these high levels of NO is not a diffusion flame (which would have a low MPRR), but a bulk reaction at close to stoichiometric composition.

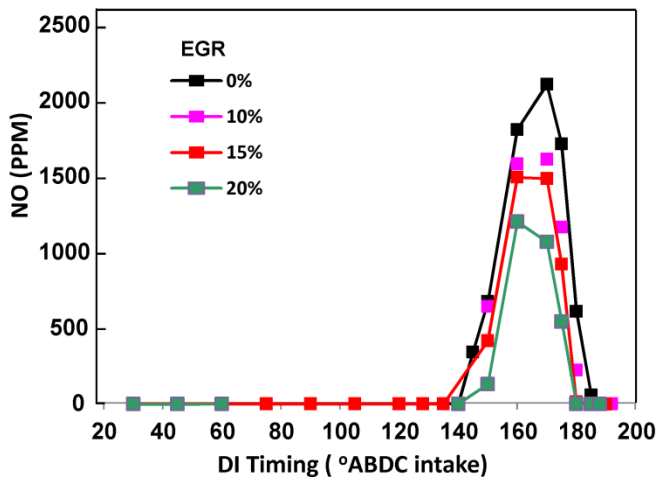


Figure 8 NO emissions corresponding to the data in Figure 3.

Discussion

There are two aspects to be explained in the observed behavior of the effect of SOI of the DI fuel on combustion:

- The combustion phasing behaviors: that with retard of SOI, combustion first retards in regime A, and then advances in regime B, and finally retards in regime C.
- The MPRR behavior, which, as SOI is retarded, decreases in regime A, increases in regime B, and then decreases in regime C.

The ignition of the injected fuel is a complex process involving fuel atomization, evaporation, mixing with the hot charge, and the cumulative chemical reactions leading to the major heat release event. The interaction of the concentration field, which is governed by the mixing process, and the pre-combustion temperature field, which is mainly governed by the piston motion, significantly impacts the ignition delay. The process is further complicated by the local cooling of the charge by fuel evaporation.

That the SOI of the DI fuel affects the ignition and combustion behaviors is due to the influence on these behaviors by the fuel concentration. The PFI fuel is relatively well mixed. By itself, this lean mixture ($\Phi = 0.24$ to 0.3) has a long ignition delay. Therefore, the ignition and combustion behaviors are determined, for the early direct injection cases, largely by the timing of the directly injected fuel.

The SOI of the DI fuel and CA 10 are shown in Figure 9. Also shown in the figure are the representative temperature and pressure of the charge into which the DI fuel is injected. The injection duration is short (2.8 CA-deg) compared to the compression and expansion processes so that the fuel could be visualized as a puff of droplets collectively going through evaporation, mixing, and pre-ignition chemistry. The CA10 point indicates the beginning point of significant heat release so that the time between SOI and CA10 may be interpreted as the ignition delay.

In regime A, the injection goes into a charge of low temperature and pressure. The ignition delay is long. When SOI is retarded from point P to point Q, ignition delay decreases because fuel is injected into a denser and hotter environment, both of which promote evaporation and chemistry, and hence a reduction in the ignition delay. The shortening of the ignition delay, however, is not enough to compensate for the retard of SOI. The net result is that ignition, and hence CA10, retards with retard of SOI.

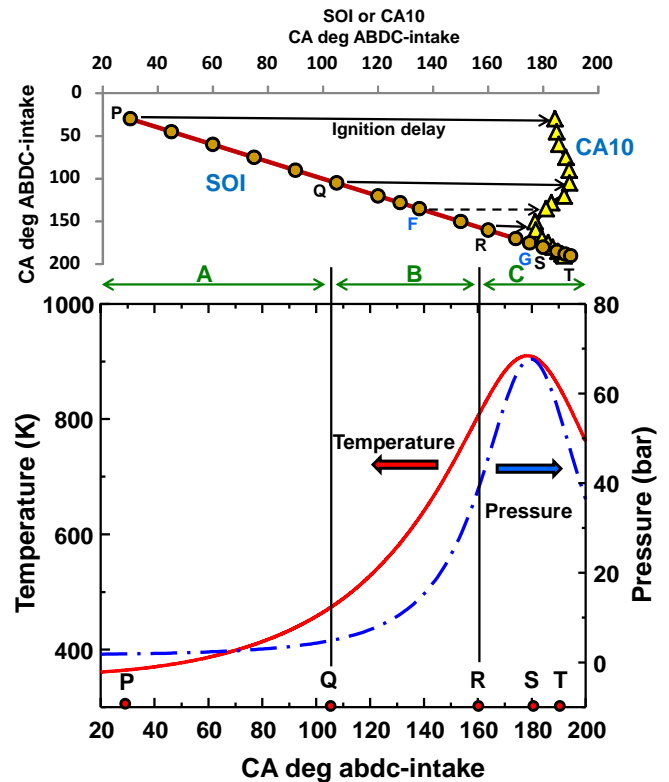


Figure 9 SOI of the DI fuel and CA10. Also shown are the compression temperature and pressure; 1200 rpm; 1.8 bar MAP; EGR=15%; $\Phi = 0.33$. Values are representative values of the charge into which the DI fuel is injected. The points P, Q, R, S, and T correspond to those in Figure 3.

In regime B, fuel is injected into a much hotter and denser environment; hence the ignition delay is shorter. The sensitivity of the ignition delay to fuel equivalence ratio may further play a role: the fuel is more stratified here than in regime A; the fuel rich regions in the high temperature environment have a shorter ignition delay. The shortened delay over compensates for the later SOI. Thus, when SOI is retarded from point Q to point R, the net effect of the shorter ignition delay and later injection results in advancement of ignition and CA10.

In regime C, the ignition delay becomes very short. The time required to physically prepare the mixture (evaporation and mixing) overpowers the gain in shortening the delay because of the hotter and denser charge and because of stratification. Thus the trend reverses again: the combustion retards with the retard of SOI. (For the last four points (from S to T) of the data set, the PFI fuel ignites before SOI of the DI fuel.)

It has been pointed out earlier that for the EGR=20% case, the combustion becomes unstable first when SOI is later than 60° ABDC-intake, and becomes stable again when SOI is further retard to beyond 140° ABDC-intake. The former behavior is due to that the ignition is progressively late in regime A; when it is sufficiently late into the expansion stroke, the charge may fail to ignite and the combustion becomes unstable since the charge temperature is progressively lower in the expansion process. When SOI is retarded to beyond 140° in regime B, however, the ignition delay becomes shorter due to the injection into a hotter charge; this effect compensates for the late SOI (regime B). Then combustion commences earlier and stabilizes.

The above discussion explains the change in combustion phasing as a function of SOI is a result of the competition between the change in ignition delay and the retard of SOI. The effect of SOI on MPRR is discussed next.

With SOI retard, the MPRR first decreases in regime A, then increases sharply in regime B, and then decreases again in regime C (Figure 3). When MPRR is plotted against CA50, however, the curve is monotonic. This is shown in Figure 10. There appears to be two “branches” of data. The upper branch comprises data from regime C; the lower one from regime B and A. This observation will be discussed later.

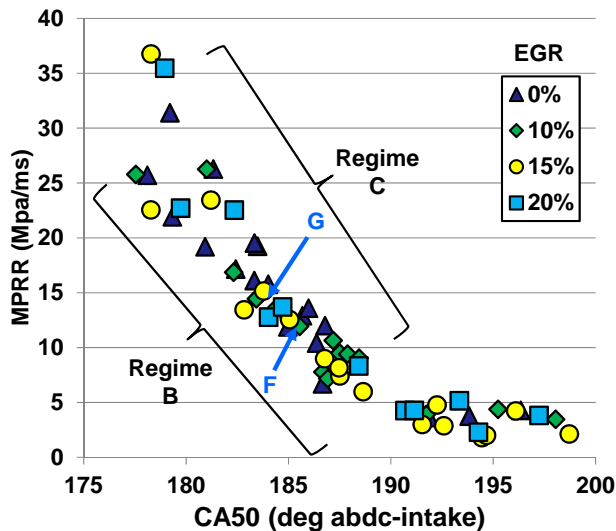


Figure 10 MPRR as a function of CA50; data correspond to those in Figure 3. The splitting of the data into two branches corresponds to combustion in regimes B and C; the latter has the higher MPRR values.

The pressure rise rate is determined by the net heat release rate and the volume expansion of the cylinder. Using a perfect gas model for the charge, the relationship is

$$\dot{p} = \frac{(\gamma - 1)\dot{q}}{V} - \gamma p \frac{\dot{V}}{V} \quad (1)$$

The volume expansion term (last term in Eq. (1)), is small. For example, at point Q in Figure 3, CA50 is at 195° ABDC-intake. Assuming a nominal pressure of 100 bar, this term is then -0.3

MPa/ms. Going from point P to point Q in Figure 3, the MPRR drops from 9 MPa/ms to 1.8 MPa/ms (factor of 5). Therefore, this term can be neglected.

The larger V in the first term of Eq. (1) would also result in a decrease of the MPRR. Although the change in V from TDC to 195° ABDC-intake (CA50 of point Q in Figure 3) is substantial (30.6%), it is still negligible in terms of explaining the factor of 5 drop in MPRR going from P to Q. Thus the change in MPRR has to come from the reduction of \dot{Q}

The conventional wisdom is that the relaxing for \dot{Q} is a result of charge stratification (by fuel concentration and/or temperature gradients) so that the charge is sequentially ignited. The above data, however, indicate otherwise. For example, consider points F and G (shown in Figures 3, 9, and 10); they are in regimes B and C respectively. The pertinent combustion parameters for these points are shown in Table 4. The ignition delay, defined as the difference between CA10 and SOI, are vastly different (55° CA in F and 7° CA in G); hence the fuel stratification should be very different because of the difference in evaporation and mixing time. Yet the two points have approximately the same MPRR. Therefore using fuel stratification to explain the behavior would not fit.

Another explanation is that with later combustion phasing, temperature stratification increases, thereby enhancing the sequential burning process and lowers the MPRR. The data in Figure 10 shows a decrease of MPRR by roughly a factor of 6 with a CA50 retard of 10°, which, at 1200 rpm, corresponds to 1.4 ms. It is unlikely that the temperature profile will change substantially in such a short time. Furthermore, the piston is close to top dead center for the high MPRR values in Figure 10 so that temperature profile change due to volumetric expansion is insubstantial. Therefore, an alternative mechanism has to be sought.

Table 4 Combustion parameters for points F and G in Figures 3, 9, and 10; crank angles referenced to ABDC-intake. Engine operates at 15% EGR.

Point	SOI	CA10	CA50	MPRR (MPa/ms)
F	128°	183°	185°	12.5
G	175°	182°	184°	15.2

To explain the data, it is proposed that the heat release process is mostly a bulk one instead of a sequential one, with a finite reaction rate which is sensitive to temperature, although at high temperature (where the MPRR is large), sequential combustion due to temperature gradient may still take place. It will be shown in the next section that from the RCM data, ignitions in the engine mostly take place in the negative temperature coefficient (NTC) region so that sequential ignition by temperature gradient mechanism is suppressed. In Figure 11, the MPRR values are plotted against the unburned gas temperature at CA10 (at which, the heat release is still small so that the charge temperature is governed mainly by the compression process). The unburned gas temperature is calculated by a cycle simulation. The collapse of the data points lends support to the hypothesis.

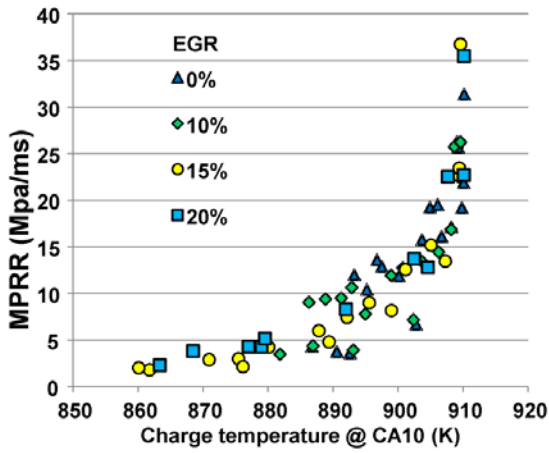


Figure 11 MPRR as a function of the charge temperature at CA10.

The charge stratification, however, does have a secondary effect on the combustion:

- The region with the higher Φ does burn faster. Thus the more stratified cases have a higher MPRR and combustions in regime C (more stratified) at the same CA50 has higher MPRR values than those in regime B. As a result, the MPRR as a function of CA50 in Figure 10 exhibits two branches, with the regime C data comprising the upper branch. (That the two branches do not show up in the MPRR versus charge temperature at CA10 in Figure 11 is because at the higher MPRR values where the two branches significantly differ, CA10 values are close to TDC and the charge temperatures do not change appreciably.)
- The stratified charge produces regions of Φ close to stoichiometric. There is significant NO production in the hot burned gas in these regions; hence the high NO emission as shown in Figure 8. When the data are plotted versus CA50 (Figure 12), the results also show two branches, corresponding to regimes B and C. There is more stratification in the latter, resulting in a higher NO emission.

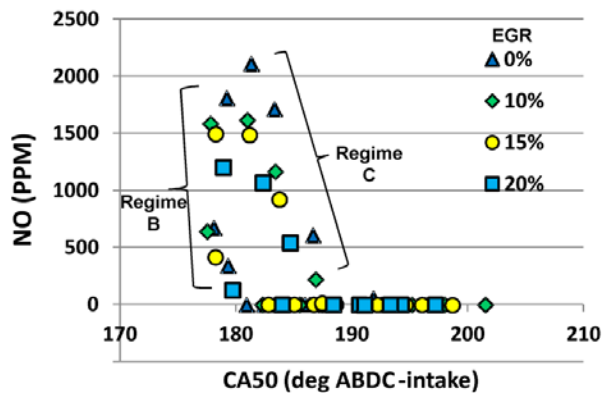


Figure 12 NO versus CA50 for the data in Figure 8.

To confirm indeed that it is possible to have a bulk heat release with a finite rate that is sensitive to the temperature, combustion experiments have been carried out in a rapid

compression machine. The results are described in the next section.

Rapid Compression Machine results

When the engine is operating at 15% EGR, the exhaust Φ is 0.5. Then when the oxygen in the recirculated burned gas is accounted for, the unburned gas Φ of the trapped charge is 0.43. To simulate conditions representative of the engine environment, the RCM is operated with the Halterman 437 fuel at $\Phi = 0.4$, at a fixed compressed charge density of 0.7 kmol/m^3 , and with the air diluted 15% by mole with nitrogen. The compressed density is 30% lower than the peak compressed density ($\sim 0.9 \text{ kmol/m}^3$) in the engine because of hardware limitation (the peak combustion pressure would be too high for the apparatus.) Therefore the ignition delay and the MPRR values obtained from the RCM will be respectively longer and lower than those encountered in the engine at the same temperatures. Nevertheless, the results should still give insight to the nature of the combustion of a homogeneous charge at conditions similar to those of the engine. The ignition delay and the rate of pressure rise are measured for a range of compression temperatures.

The pressure traces of this set of RCM experiments are shown in Figure 13. (Different compression ratios: 12, 18 and 20, are used to obtain the compression temperatures; therefore the compression parts of the pressure traces are different.) The pressure traces show two stage ignitions with a cool flame period followed by the main heat release. The pressure rise rate associated with the main heat release is of the order of milliseconds. The mixture has been premixed (stirred with an internal fan in a mixing chamber for a few minutes) and therefore, should be uniform. An upper bound for the thermal boundary layer thickness is of the order of 0.2 mm (for a boundary layer growth period of 30 ms); the value is small compared to a clearance height of 1 cm (at CR = 20). Therefore, there should be a substantial core gas with uniform temperature. The absence of significant concentration and temperature gradients in the core gas indicates a bulk heat release reaction which takes place at a finite time of a few milliseconds.

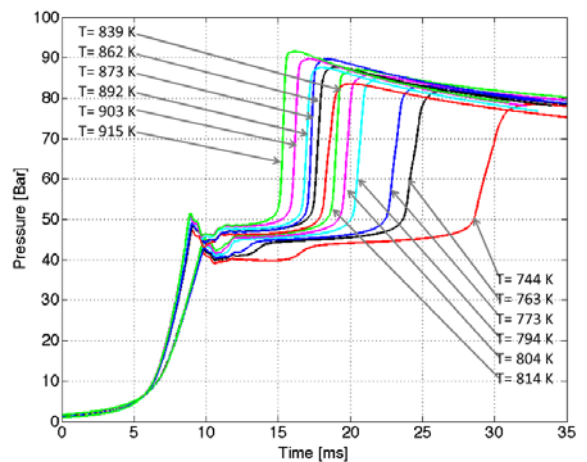


Figure 13 Pressure traces from temperature sweep in RCM experiments; $\lambda = 0.4$, air diluted 15% with N_2 ; compressed density = 0.7 kmol/m^3 .

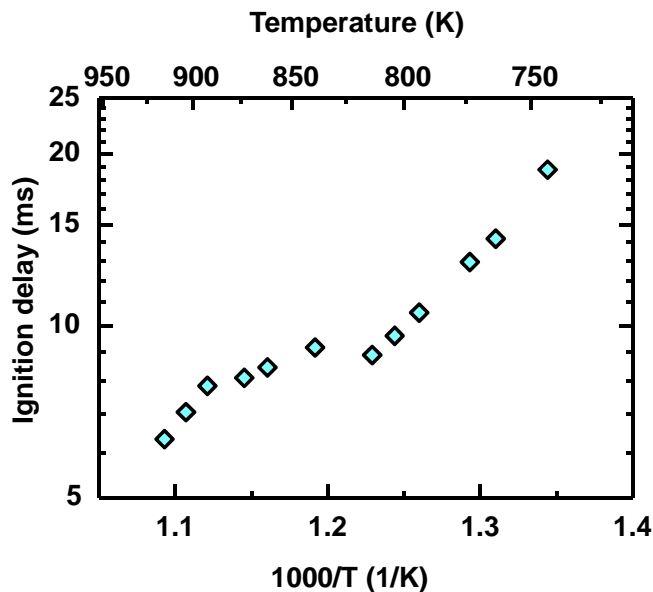


Figure 14 Ignition delay from RCM data of Figure 13.

The ignition delay as a function of temperature is shown in Figure 14. The temperature at CA10 for the engine experiment is between 860 K and 910 K; see Figure 11. Thus the engine ignitions mostly occur in the negative temperature coefficient region and are not sensitive to temperature. Hence the mechanism for sequential ignition via temperature gradient is suppressed. However, it should be noted that the RCM data have been obtained at a charge density which is 30% lower than the peak compressed density in the engine; thus the ignition curve relevant for the engine should shift down and to the right of the data points in Figure 14. Then combustion at the higher temperatures where MPRR is high could move from the NTC region to the high temperature region where ignition delay is sensitive to temperature and sequential burning could occur.

The maximum pressure rise rate, which is an indicator of the heat release rate, from the RCM data is shown in Figure 15. The rate increases almost linearly with the temperature. The engine data in Figure 11, however, have shown more sensitivity to temperature. One factor for the difference is due to that the RCM experiments have been done at a fixed compressed density, while the density of the charge at combustion changes with combustion phasing. The engine results shown in Figure 11 are thus a combined effect of temperature and density changes. The MPRR dependence on temperature observed in the engine experiments (Figure 11) is therefore consistent with the finite heat release rate that increases with temperature observed in the RCM experiment.

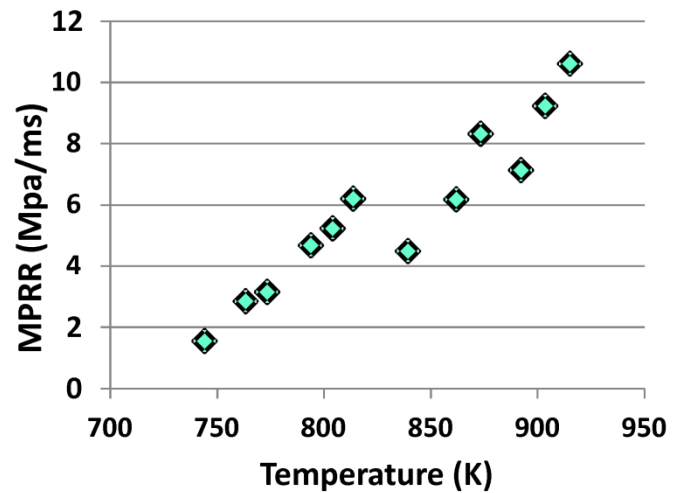


Figure 15 MPRR from RCM data of Figure 13.

Results from other split injections

To illustrate the effect of stratification, different proportion of the PFI/DI fuel is used. The MPRR values versus CA50 for PFI/DI split of 80/20 are shown in Figure 16. Compared to the results of the 60/40 split (Figure 10), the difference in MPRR in regime B and C for the same CA50 is much less. This observation is consistent with the explanation that the difference is a result of the fuel stratification, which is made smaller when the DI fuel is reduced.

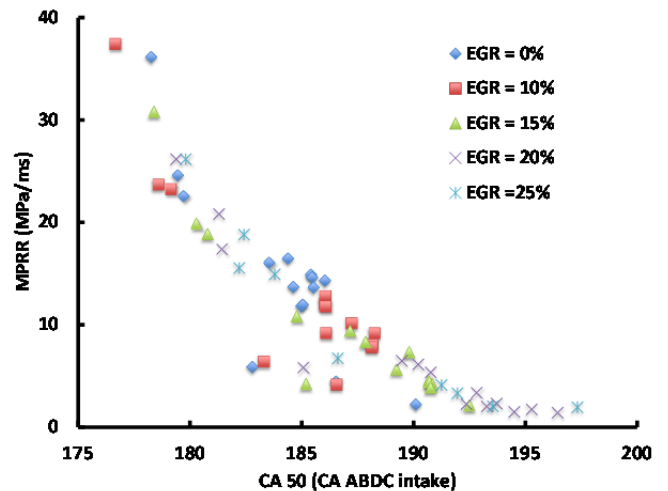


Figure 16 MPRR versus CA50; PFI/DI split of 80/20; 1200 rpm, 23 mg fuel.

To accentuate the effect of stratification, the PFI/DI split is changed to 40/60. Then the MPRR for the same CA50 diverges substantially between regimes B and C; see Figure 17. This observation is consistent with that when there is more DI fuel, the stratification would be enhanced.

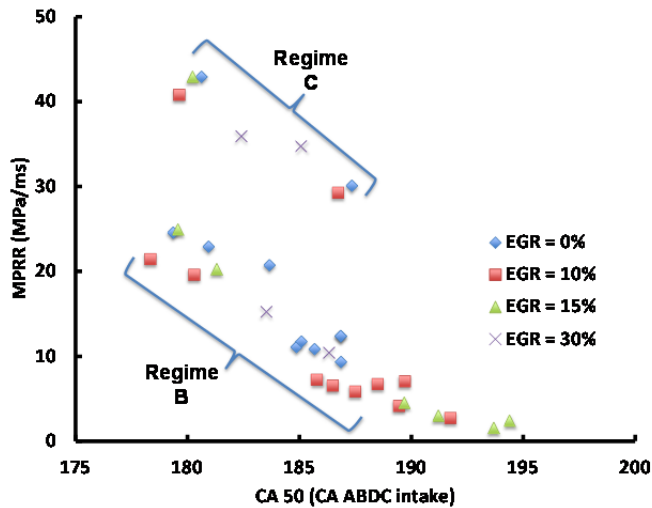


Figure 17 MPRR versus CA 50; PFI/DI split of 40/60; 1200 rpm, 23 mg fuel.

Figure 18 shows the MPRR for PFI/DI split of 0/100 (i.e. only DI). The split of the MPRR values at the same CA50 is consistent with that of the other cases.

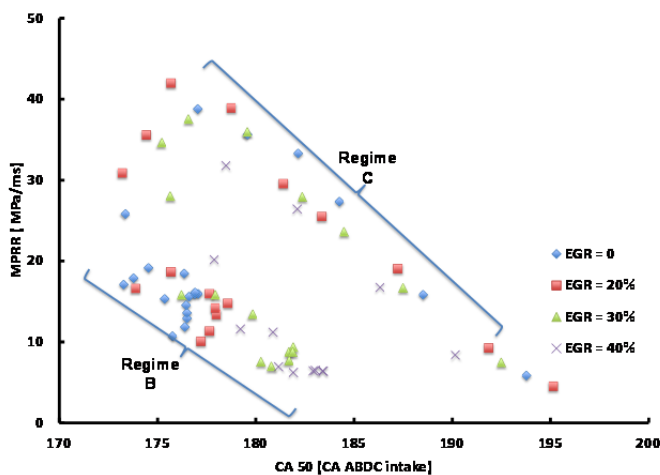


Figure 18 MPRR versus CA 50; 100% DI fuel; 1200 rpm, 23 mg fuel.

Summary/Conclusions

The nature of heat release in gasoline partially premixed compression ignition (PPCI) engine has been investigated in a gasoline engine equipped with both port-fuel-injection (PFI) and direct injection (DI). Fuel introduced in the former provides a uniformly mixed mixture into which the DI fuel is introduced at different time during the compression process. The following observations are made.

- As the start of injection (SOI) of the DI fuel is retarded from early compression, the maximum pressure rise rate (MPRR) first decreases, then increases substantially, and decreases again.

- The crank angle at 50% mass fraction burn (CA50) first retards, then advances, and then retards again correspondingly.
- The MPRR correlates mostly with the combustion phasing which changes the mixture temperature at combustion.
- The primary effect of SOI is to change the combustion phasing, and the MPRR responds to the combusting phasing change. Thus a relatively well mixed mixture (with early injection) and a much stratified mixture (with late injection) could have the same MPRR.
- The observation is explained by a bulk heat release process, of which the rate increases with temperature, rather than by a sequential ignition process
- Observations from the compression ignition of homogeneous charges in a Rapid Compression Machine support this explanation.
- A secondary effect of the SOI timing is that a later injection produces a more stratified charge and leads to a higher MPRR because locally richer regions burns faster.

References

- Kalghatgi, G., Risberg, P., and Ångström, H., "Advantages of Fuels with High Resistance to Auto-ignition in Late-injection, Low-temperature, Compression Ignition Combustion," SAE Technical Paper 2006-01-3385, 2006, doi:10.4271/2006-01-3385.
- Kalghatgi, G., Risberg, P., and Ångström, H., "Partially Pre-Mixed Auto-Ignition of Gasoline to Attain Low Smoke and Low NOx at High Load in a Compression Ignition Engine and Comparison with a Diesel Fuel," SAE Technical Paper 2007-01-0006, 2007, doi:10.4271/2007-01-0006.
- Sjöberg, M. and Dec, J., "Smoothing HCCI Heat-Release Rates Using Partial Fuel Stratification with Two-Stage Ignition Fuels," SAE Technical Paper 2006-01-0629, 2006, doi:10.4271/2006-01-0629.
- Dec, J., Yang, Y., and Dronniou, N., "Boosted HCCI - Controlling Pressure-Rise Rates for Performance Improvements using Partial Fuel Stratification with Conventional Gasoline," SAE Int. J. Engines 4(1):1169-1189, 2011, doi:10.4271/2011-01-0897.
- Noehre, C., Andersson, M., Johansson, B., and Hultqvist, A., "Characterization of Partially Premixed Combustion," SAE Technical Paper 2006-01-3412, 2006, doi:10.4271/2006-01-3412.
- Leermakers, C., Luijten, C., Somers, L., Kalghatgi, G. et al., "Experimental Study of Fuel Composition Impact on PCCI Combustion in a Heavy-Duty Diesel Engine," SAE Technical Paper 2011-01-1351, 2011, doi:10.4271/2011-01-1351.
- Shen, M., Tuner, M., Johansson, B., and Cannella, W., "Effects of EGR and Intake Pressure on PPC of Conventional Diesel, Gasoline and Ethanol in a Heavy Duty Diesel Engine," SAE Technical Paper 2013-01-2702, 2013, doi:10.4271/2013-01-2702.
- Inagaki, K., Fuyuto, T., Nishikawa, K., Nakakita, K. et al., "Dual-Fuel PCI Combustion Controlled by In-

Cylinder Stratification of Ignitability," SAE Technical Paper 2006-01-0028, 2006, doi:10.4271/2006-01-0028.

9. Kokjohn, S., Hanson, R., Splitter, D., and Reitz, R., "Experiments and Modeling of Dual-Fuel HCCI and PCCI Combustion Using In-Cylinder Fuel Blending," SAE Int. J. Engines 2(2):24-39, 2010, doi:10.4271/2009-01-2647.
10. Leermakers, C., Van den Berge, B., Luijten, C., Somers, L. et al., "Gasoline-Diesel Dual Fuel: Effect of Injection Timing and Fuel Balance," SAE Technical Paper 2011-01-2437, 2011, doi:10.4271/2011-01-2437.
11. Maria, A., Cheng, W., Kar, K., and Cannella, W., "Understanding Knock Metric for Controlled Auto-Ignition Engines," SAE Int. J. Engines 6(1):533-540, 2013, doi:10.4271/2013-01-1658.
12. Maria, A., "On Fuel Selection in Controlled Auto-Ignition Engines: the Link Between Intake Conditions, Chemical Kinetics, and Stratification," PhD thesis, Dept. of Mech. Eng., MIT, 2012.

Contact Information

Prof. Wai Cheng, MIT; wkcheng@mit.edu

Acknowledgments

The research has been supported by the US Department of Energy University Consortium on High Pressure Lean Combustion. The members are MIT, University of Michigan and University of California, Berkeley.

Definitions/Abbreviations

ABDC-intake	After bottom dead center of intake stroke	q	Heat release
CR	Compression ratio	RCM	Rapid compression machine
DI	Direct injection	Regime A	Range of injection sweep in which the MPRR decreases with SOI retard; see Fig. 3
EGR	Exhaust gas recirculation	Regime B	Range of injection sweep in which the MPRR increases with SOI retard after regime A; see Fig. 3
MPRR	Maximum pressure rise rate	Regime C	Range of injection sweep in which the MPRR decreases with SOI retard after regime B; see Fig. 3
GIMEP	Gross indicated mean effective pressure	RON	Research octane number
MPU	Mixing preparation unit	SOI	Start of injection
MON	Motor octane number	V	Volume of combustion chamber
NTC	Negative temperature coefficient	γ	Specific heat ratio
p	Pressure	λ	Air fuel equivalence ratio
PFI	Port fuel injection	Φ	Fuel air equivalence ratio
PPCI	Partially premixed compression ignition		